IEEE Access
Multidisciplinary | Rapid Review | Open Access Journal

Received 8 August 2022, accepted 29 August 2022, date of publication 1 September 2022, date of current version 16 September 2022.

Digital Object Identifier 10.1109/ACCESS.2022.3203730

RESEARCH ARTICLE

Optimized Two-Level Control of Islanded Microgrids to Reduce Fluctuations

EHSAN AKBARI[1], NIMA SHAFAGHATIAN[2], FARHAD ZISHAN[3], OSCAR DANILO MONTOYA[4,5], AND DIEGO ARMANDO GIRAL-RAMÍREZ[6]

[1]Department of Electrical Engineering, Mazandaran University of Science and Technology, Babol 4515613191, Iran
[2]Electrical Engineering Department, Zanjan University, Zanjan 3879145371, Iran
[3]Department of Electrical Engineering, Sahand University of Technology, Tabriz 5331817634, Iran
[4]Grupo de Compatibilidad e Interferencia Electromágnetica, Facultad de Ingeniería, Universidad Distrital Francisco José de Caldas, Bogotá 110231, Colombia
[5]Laboratorio Inteligente de Energía, Facultad de Ingeniería, Universidad Tecnológica de Bolívar, Cartagena 131001, Colombia
[6]Ingeniería Eléctrica, Facultad Tecnológica, Universidad Distrital Francisco José de Caldas, Bogotá 110231, Colombia

Corresponding authors: Nima Shafaghatian (nima.shafaghatian@znu.ac.ir), Farhad Zishan (f_zishan99@sut.ac.ir), and Oscar Danilo Montoya (odmontoyag@udistrital.edu.co)

ABSTRACT The main problem in the operation of micro-grids is controlling the voltage and frequency. The inertia of the whole grid is low, so the operation of the system is interrupted by sudden changes in load or incidence in the absence of a proper control system. In order to solve this issue, various control structures have been proposed. In this paper, an optimal distributed control strategy for coordinating multiple distributed generation instances is presented in an islanded microgrid. A secondary frequency control method is implemented in order to eliminate voltage deviation and reduce the small signal error. In this layer, an optimized PID controller is used. PID controller optimization is carried out via the Honey Badger Algorithm, and results are obtained using the MATLAB software. According to the results, inadequate adjustment of a secondary loop leads to poor and unacceptable outcomes, and the necessary power quality is not achieved. However, by using the proposed method, a proper performance of the microgrid in the face of disturbances is achieved.

INDEX TERMS Microgrids, two-level control, optimization, distributed control, honey badger algorithm.

I. INTRODUCTION

Microgrids have been proposed as a substitute for traditional power systems due to their benefits. These systems include distributed generation sources, inverters, storage equipment, and a control system, which is responsible for providing sensitive and insensitive loads in often sensitive locations such as hospitals. The main objectives of using microgrids are increasing reliability, reducing casualties and environmental pollution, obtaining a variety of economic benefits, among others. The main issue with exploiting these systems is controlling the voltage and frequency. In [1] and [2], microgrids were introduced as a suitable substrate for the use of renewable energy. Under normal conditions, microgrids are connected to the main grid. If necessary, microgrids must be separated from the network and can independently supply their attached loads (island mode). In [3] and [4], solutions for detecting the isolation mode were proposed. Thereupon, a microgrid should be able to work in both connected and island mode. For each of these modes, various control structures have been presented. In [5], [6], and [7], PQ control for the network-connected mode was proposed. Given that, in this case, the voltage and frequency are provided by the main network, only adjusting the grid's overlapping power and applying proper power sharing are required. However, more challenges arise in islanded mode, such as controlling and adjusting the basic parameters of the system. Various control structures have been proposed for this mode. There are many techniques for controlling parallel inverters that can be divided into three categories: 1) master/slave control, 2) feedback-based methods, and 3) droop control methods.

Each of these methods has its advantages and disadvantages. In master/slave methods, the inverter does not require a PLL circuit, and load flowing is carried out as well.

The associate editor coordinating the review of this manuscript and approving it for publication was Inam Nutkani.

Moreover, the impedance of the communication line between the inverters does not affect the control operation (unlike droop-based methods), and the system is easily promoted. However, this method also has disadvantages. By increasing the number of slaves, the stability of the system is reduced, and the frequency suffers from ripples [8]. In addition, this control method requires control communication between components, which implies lower reliability.

On the other hand, feedback-based methods have many benefits. The transient responses are usually good in these methods, the control process is based on local measurements, and there is a high reliability due to the lack of a communication system. However, these systems are not easy to upgrade and usually cannot be counted among plug-and-play systems.

Droop control-based methods have also been widely used [9], [10]. The prohibitions of these techniques are the impact of the reactive power from line impedance. To overcome this problem, a method in was proposed by [11]. Another limitation is that, after load changes, these control methods do not necessarily return the system to nominal values. To solve this problem, a secondary control loop is typically used. Furthermore, in light of severe disturbances, this layer reduces the transients and maintains the main parameters of the voltage and frequency at the lowest time to nominal values. This control methodology usually receives feeds from load voltage and frequency [12], [13].

In the simplest case, a feedback control is used. Regulation is performed by comparing a reference to the error signal, which is sent to the controller. Then, the controller sends the signals required to produce an inverter signal, which is usually a PWM or a hysteresis loop. The controller is usually a PI or PID controller, whose coefficients can be adjusted in different ways. This control is usually entrusted with large signal error conditions. The most popular method for the secondary control loop involves PID controllers, but adjusting the coefficients of these controllers becomes the next challenge. There are several ways to do this. In [14], these controllers were set via the Ziegler-Nichols method, but this did not result in the optimal operation. Therefore, newer practices were also provided to this effect. In [15], a technique based on the famous geographic method was proposed. This control method reduces the transient courier under error conditions. Considering the frequency response of inverter controllers, as well as the rapid changes under said conditions, these devices were not able to quickly reduce the error flow [16]. The transient process of the inverter remained in the first cycle, and the scope of these changes was incremental. Therefore, if these changes are converted to a range of reference voltage changes, along with a negative sign to other control circles that make voltage reference changes, the controller can be made faster. Management of the control parameters can be implemented so that they do not have an effect on the system.

This control method also is used to create small signal stability. To design it, a complete dynamic model of the system along with all its components should be derived. Then, according to the transient state response, control signals can be designed to increase system stability. In [17], the feedback control of the voltage domain was used to improve Q-V droop. Then a small signal analyze was done to test the accuracy of the proposed method. Moreover, in [18], an optimal controller coefficient adjustment method based on the small signal system model was proposed for eliminating the effect of small signal disturbances while changing the microgrid operation mode from grid-connected to islanded [19].

In this paper, an optimal distributed control strategy is presented for coordinating multiple distributed generators. A secondary control method is applied to the system in order to eliminate voltage deviation and reduce the small signal error. The second control loop is optimized via the Honey Badger Algorithm (HBA). Unlike previous methods, this one provides references for voltage and frequency, and it applies power sharing, controls the system in the face of severe changes, and prevents severe fluctuations. A novel, recently presented algorithm is also used to adjust the controller's coefficients. The results are compared with Black Widow Optimization (BWO) and PSO algorithms.

In selecting these 3 algorithms some tips were taken into account. These algorithms represent different categories of meta-heuristics. PSO is a stochastic optimization technique based on the movement and intelligence of swarms. It is also one of the old and authentic algorithms that is used as a benchmark for measurement and comparison. This algorithm is based on collective intelligence. BWO like PSO, is one of the bioinspired algorithms but uses exploration and exploitation to find the optimum solution. HBA is one of the trajectory algorithms. As a result, the best group of algorithms that are suitable for optimizing the proposed problem and the effect of the optimized secondary control loop can be seen.

Therefore, the innovation presented in this article can be defined as follows:

- Optimizing the second control loop of microgrids and checking its effect on power quality
- Applying optimization with two different categories of meta-heuristic algorithms and determining the best category of algorithms in this type of problem.

All optimization processes and simulations are performed using the MATLAB software.

The rest of this article is organized as follows: Section II describes the first-level control; Section III is dedicated to the secondary control; Section IV presents the simulation results; Section V presents the main conclusions drawn from this study.

II. OPTIMAL DISTRIBUTED CONTROL FOR ADJUSTING THE VOLTAGE AND FREQUENCY IN AN ISLANDED MICROGRID

A. GRAPH THEORY

If there is anij transmission line that connects the DGi and the DGj, the latter is located in the ni neighborhood, which represents J $\in$ ni. DGi can only receive information from the

ni neighborhood with a dij > 0 communication coefficient. Otherwise, dij = 0. If any DG unit is considered to be nodes and transmission lines to the edges, the topology of a microgrid can be regarded as a graph. If dij = dji, the graph is without direction. If there is a path that connects both separate units, the graph is attached. dii is the distance of units as described below:

$$\mathrm{d_{ii}} = -\sum\nolimits_{\mathrm{j}\in \mathrm{N_i}} \mathrm{d_{ij}}, \mathrm{j} \neq \mathrm{I} \tag{1}$$

The Laplace matrix is D = [dij]. Suppose that the special values of the Laplace matrix are arranged in an increasing form. Then, the following relationship is valid [20]:

$$|\lambda_n| \geq \ldots \geq |\lambda_2| > |\lambda_1| = 0, |\lambda_i| \leq 0, \forall i = 1, 2, \ldots, n \tag{2}$$

For a non-directional graph, the following characteristics are valid [21]:

$$\sum_{i,j=1}^{n} d_{ij} x_i sign\left(x_j - x_i\right) \left|x_j - x_i\right|^k = -\frac{1}{2} \sum_{i,j=1}^{n} d_{ij} \left|x_j - x_i\right|^{1+k} \tag{3}$$

$$\mathrm{x^T} Dx = \frac{1}{2} \sum\nolimits_{i,j=1}^{\mathrm{n}} \mathrm{d_{ij}} (x_j - x_i)^2,$$

$$x^T D^2 x = \frac{1}{2} \sum\nolimits_{i,j=1}^{\mathrm{n}} \mathrm{d_{ij}^2} (x_j - x_i)^2 \tag{4}$$

$$\mathrm{x^T} Dx \geq \lambda_2 (D) x^T x \tag{5}$$

$$\mathrm{x^T} (D + C) x = \frac{1}{2} \sum\nolimits_{i,j=1}^{\mathrm{n}} \mathrm{d_{ij}} (x_j - x_i)^2 + c_i \sum\nolimits_{\mathrm{i}=1}^{\mathrm{n}} x_i^2 \tag{6}$$

$$\mathrm{x^T} (D + C) x \geq \lambda_1 (D + C) x^T x \tag{7}$$

where $x = \{x_1, \ldots, x_n\}$ is the state variable that should be exchanged between the neighboring DG units, ci is the interest pinning, $c = \mathrm{diag}\ \{c_1, \ldots, c_n\}$, λ_2 is the second smallest eigenvalue of D which is also returned to algebraic connection D and λ_1 is the smallest eigenvalue of $(D + C)$.

B. OPTIMAL CLOSED-LOOP CONTROL ALGORITHM

A nonlinear dynamical system is considered as follows:

$$\dot{x}(t) = f(x) + G(x) u(t) = F(x), x(0) = x_0 \tag{8}$$

The performance index is expressed as follows:

$$J = \min_{x,u} \int_0^\infty L(x, u)\, dt = \min_{x,u} \int_0^\infty L_1(x) + u^T(x) Ru(x)\, dt \tag{9}$$

where L_1 is a criterion for the mode variable, and $R = \mathrm{diag}\ \{R_1 \ldots R_n\}$, with R_i as control input weight. The Hamiltonian function [22] is defined as follows:

$$H(x, u) = L(x, u) + S(x) F(x) \tag{10}$$

where $S(x)$ is a common variable set. Optimal control is designed to minimize the Hamiltonian function, which is shown below:

$$u = arg \min_{x,u} \{L(x, u) + S(x) F(x)\} \tag{11}$$

The necessary condition for validating Eq. (11) is the first-order derivative of (10) with respect to u is zero:

$$\frac{\partial H}{\partial u} = \frac{\partial}{\partial u} \left[L_1(x) + u^T Ru + S(x)(f(x) + G(x) u)\right] = 0 \tag{12}$$

The optimal u control law can be obtained from Eq. (12).

$$u = -\frac{1}{2} R^{-1} [S(x) G(x)]^T \tag{13}$$

The Hamilton-Jacobi-Bellmen steady-state equation (8) has been considered for uncontrolled nonlinear dynamic systems by [23]:

$$\begin{aligned} &L(x, u) + S(x) F(x) \\ &= L_1(x) + S(x) f(x) \\ &\quad -\frac{1}{4} [S(x) G(x)] . R^{-1} [S(x) G(x)] = 0 \end{aligned} \tag{14}$$

Therefore,

$$L_1(x) = \frac{1}{4} [S(x) G(x)] . R^{-1} [S(x) G(x)] - S(x) f(x) \tag{15}$$

Suppose there is a continuous differential function of Lyapanov $V(x) > 0$ that provides the following conditions:

$$\frac{dV(x)}{dt} = \frac{dV(x)}{dx} \frac{dx}{dt} = S(x) F(x) \tag{16}$$

$$\frac{dV(x)}{dt} \leq -\rho (V(x))^\alpha, \rho > 0, 0 < \alpha < 1 \tag{17}$$

in a nonlinear system, the zero solution is finite-time stable if there exists an open neighborhood of the origin and a function tends to zero, called the settling-time function. On the other hand, system (8) is globally under the control of control law (13), which meets the following conditions [23]:

$$\lim_{t \to T} V(x(t)) = 0 \quad V(x(t)) = 0, \forall t \geq T \tag{18}$$

with the limited adjustment time function given by

$$T \leq \frac{1}{\rho (1 - \alpha)} (V(x_0)^{1-\alpha} \tag{19}$$

C. SUGGESTED DISTRIBUTED CONTROL

Consider an islanded microgrid consisting of several inverter-based DGs. Each DG unit is composed of a DC voltage source, a voltage source inverter (VSI) [19], and an inductive-capacitive-inductive filter, as shown in Fig 1.

Power sharing rules allow active and reactive power to be shared based according to the DG capabilities determined by droop settings:

$$\omega_{ni} = \omega_i + m_{Pi} P_i \tag{20}$$

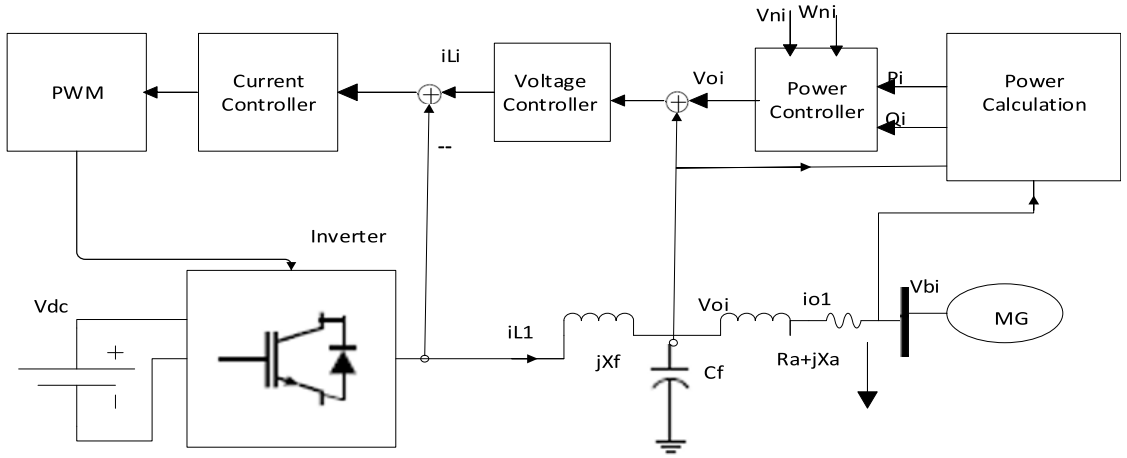

FIGURE 1. Block diagram of the control system.

$$V_{ni} = V_{oi} + m_{Qi}Q_i \tag{21}$$

where ω_{ni} and V_{ni} are designated points for frequency and voltage; ω_i and V_{ni} are the frequency and voltage of DG_i, respectively; m_{Pi} and m_{Qi} are the frequency loss and DG_i voltage. The total droop coefficient is in accordance with $m_{Pi} = \Delta\omega / P_i$ Max, and $m_{Qi} = \Delta V / Q_i$ max with the maximum acceptable frequency and magnitude deviation of $\Delta\omega$ and ΔV. The initial control cannot eliminate the frequency and voltage deviation, as this must be done by the secondary control. Only local and DG_iinformation are required to obtain ω_{ni} and V_{ni} in the initial control rules in Eqs. (19) and (20). By selecting the frequency change rate and the active power output as control variables:

$$\dot{\omega}_{ni} = \dot{\omega}_i + m_{Pi}\dot{P}_i = u_{\omega i} + u_{Pi} \tag{22}$$

$$\dot{V}_{ni} = \dot{V}_i + m_{Qi}\dot{Q}_i = u_{Vi} + u_{Qi} \tag{23}$$

Then, the nominal amount of frequency and voltage can be obtained by:

$$\omega_{ni} = \int_{t0}^{t} u_i^{\omega}(\tau) + u_i^{p}(\tau)\, d\tau \tag{24}$$

$$V_{ni} = \int_{t0}^{t} u_i^{V}(\tau) + u_i^{Q}(\tau)\, d\tau \tag{25}$$

The proposed control approach restores the frequency and the size of the DG voltage to the desired values and achieve exact quantitative/reactive power sharing, which is summarized as follows:

$$\lim_{t\to T_\omega} \left|\omega_i(t) - \omega^{ref}\right| = 0, \omega_i(t) = \omega^{ref}, \forall t \geq T_\omega \tag{26}$$

$$\lim_{t\to T_P} \left|\frac{P_i(t)}{P_i^{max}(t)} - \frac{P_j(t)}{P_j^{max}(t)}\right| = 0, \frac{P_i(t)}{P_i^{max}(t)} = \frac{P_j(t)}{P_j^{max}(t)}, \forall t \geq T_P \tag{27}$$

with a compromise between $\lim_{t\to\infty}\left|V_{oi}(t) - V^{ref}\right| = 0$, $\lim_{t\to\infty}\left|\frac{Q_i(t)}{Q_i^{max}(t)} - \frac{Q_j(t)}{Q_j^{max}(t)}\right| = 0$, where $\frac{P_i(t)}{P_i^{max}(t)}$ and $\frac{Q_i(t)}{Q_i^{max}(t)}$ are active and reactive proportions of DGi.

D. OPTIMAL DISTRIBUTION OF FREQUENCY CONTROL WITH LIMITED TIME AND ACTIVE CAPABILITY

Consider an islanded microgrid with n units of DG. The dynamic behavior of the frequency and active power after applying the control strategy in (26) are described according to the $\dot{X}_\omega = u_\omega$ *and* $\dot{X}_p = u_P$.

where $x_\omega = (\omega_1, \ldots, \omega_n)^T$, $x_P = \left(m_{p1}P_1, \ldots, m_{pn}P_n\right)^T$, $u^\omega = \left(u_1^\omega, \ldots, u_n^\omega\right)$, and $u^p = \left(u_1^p, \ldots, u_n^p\right)$ are Lyapunov designated as follows:

$$V_\omega = \frac{4}{k}\left|X_\omega^T D_\omega^2 X_\omega\right|^{\frac{k}{2}} + \frac{2}{k}(X_\omega - X_\omega^{ref})^T C_\omega^T (X_\omega - X_\omega^{ref})^{\frac{k}{2}} \tag{28}$$

$$V_P = \frac{4}{k}\left|X_P^T D_P^2 X_P\right|^{\frac{k}{2}} \tag{29}$$

where $D_\omega = \left[d_{\omega ij}\right]$, $C_\omega = diag\{c_{\omega i}\}$, $D_p = \left[d_{pij}\right]$, $1 < k < 2$. Partial derivations V_ω, V_P, X_ω and X_P can be calculated as follows:

$$S_{\omega i} = \frac{\partial V_\omega}{\partial x_{\omega i}} = -2\left[\sum_{j\in N_i}\left(d_{\omega ij}\right)^k \operatorname{sign}\left(\omega_j - \omega_i\right)\left|\omega_j - \omega_i\right|^{k-1} + \left(c_{\omega i}\right)^k \operatorname{sign}\left(\omega^{ref} - \omega_i\right)\left|\omega^{ref} - \omega_i\right|^{k-1}\right] \tag{30}$$

$$S_{Pi} = \frac{\partial V_P}{\partial x_{Pi}} = -2\left[\sum_{j\in N_i}\left(d_{pij}\right)^k \left|m_{Pj}P_j - m_{Pi}P_i\right|^{k-1} \operatorname{sign}\left(m_{Pj}P_j - m_{Pi}P_i\right)\right] \tag{31}$$

The optimal distributed control rule can be obtained based on Eqs. (15), (30), and (31):

$$u_{\omega i} = r_{\omega i}^{-1}\left[\left(d_{\omega ij}\right)^k \operatorname{sign}\left(\omega_j - \omega_i\right)\left|\omega_j - \omega_i\right|^{k-1} + \left(c_{\omega i}\right)^k \operatorname{sign}\left(\omega^{ref} - \omega_i\right)\left|\omega^{ref} - \omega_i\right|^{k-1}\right] \tag{32}$$

$$u_{pi} = r_{pi}^{-1}\left[\sum_{j\in N_i}\left(d_{pij}\right)^k \left|m_{Pj}P_j - m_{Pi}P_i\right|^{k-1} \text{sign}(m_{Pj}P_j - m_{Pi}P_i)\right] \quad (33)$$

Inspired by [22], the proof of limited time convergence in the optimal distributed control is as follows: first, the frequency and active power errors are obtained.

$$e_\omega = (e_{\omega 1}, \ldots, e_{\omega n}) = \left(\omega_1 - \omega^{ref}, \ldots, \omega_n - \omega^{ref}\right) \quad (34)$$

$$e_p = \left(e_{p1}, \ldots, e_{pn}\right) = \left(m_{P1}P_1 - \frac{1}{n}\sum_{i=1}^{n} m_{Pi}P_i, \ldots, m_{Pn}P_n - \frac{1}{n}\sum_{i=1}^{n} m_{Pi}P_i\right) \quad (35)$$

The Lyapunov function is selected as follows:

$$V_2 = V_{e\omega} + V_{eP} = \frac{1}{2}\left(e_\omega^T e_\omega\right) + \frac{1}{2}\left(e_P^T e_P\right) \geq 0 \quad (36)$$

The first-order derivative is calculated as follows:

$$\begin{aligned}\dot{V}_2 &= \sum_{i=1}^{n} e_{\omega i}\dot{e}_{\omega i} + \sum_{i=1}^{n} e_{pi}\dot{e}_{pi} \\ &= \sum_{i=1}^{n} e_{\omega i} r_{\omega i}^{-1}\left[\sum_{j\in N_i}\left(d_{\omega ij}\right)^k sign(e_{\omega j} - e_{\omega i})\left|e_{\omega j} - e_{\omega i}\right|^{k-1} + (c_{\omega i})^2 sign(e_{\omega i})\left|e_{\omega i}\right|^{k-1}\right] \\ &\quad + \sum_{i=1}^{n} e_i^p r_{pi}^{-1}\left(d_{Pij}\right)^k sign\left(e_{Pj} - e_{Pi}\right)\left|e_{pj} - e_{pi}\right|^{k-1} \\ &\leq -\frac{1}{2}\sum_{i=1}^{n} r_{\omega i}^{-1}\left(d_{\omega ij}\right)^k \left|e_{\omega j} - e_{\omega i}\right|^k - \sum_{i=1}^{n} r_{\omega i}^{-1}\left(C_{\omega i}\right)^k \left|e_{\omega i}\right|^k \\ &\quad -\frac{1}{2}\sum_{i=1}^{n} r_{pi}^{-1}\left(d_{pij}\right)^k \left|e_{pj} - e_{pi}\right|^k \end{aligned} \quad (37)$$

According to Cauchy's inequality, the following relationship can be achieved:

$$\begin{aligned}\dot{V}_2 \leq -\frac{1}{2}&\left[\sum_{i=1}^{n} r_{\omega i}^{-\frac{2}{k}}\left(d_{\omega ij}\right)^2\left(e_{\omega j} - e_{\omega i}\right)^2 + 2\sum_{i=1}^{n} r_{\omega i}^{-\frac{2}{k}}\left(c_{\omega i}\right)^2\left(e_{\omega i}\right)^2\right]^{\frac{k}{2}} \\ &-\frac{1}{2}\left[\sum_{i=1}^{n} r_{Pi}^{-\frac{2}{k}}\left(d_{Pij}\right)^2\left(e_{Pj} - e_{Pi}\right)^2\right]^{\frac{k}{2}}\end{aligned} \quad (38)$$

According to Eqs. (5) and (7), the two terms on the right in (38) can be rewritten as follows:

$$\begin{aligned}\sigma_1 &= 2e_\omega^T R_\omega^{-\frac{2}{k}}\left(D_\omega^2 + C_\omega^2\right)e_\omega \\ &\geq 2\lambda_1\left(D_\omega^2 + C_\omega^2\right)R_\omega^{-\frac{2}{k}} e_\omega^T e_\omega \\ &= 4\lambda_1\left(D_\omega^2 + C_\omega^2\right)R_\omega^{-\frac{2}{k}} V_{e\omega}\end{aligned} \quad (39)$$

$$\begin{aligned}\sigma_2 &= 2e_P^T D_P^2 R_P^{-\frac{2}{k}} e_P \\ &\geq 2\lambda_2\left(D_P^2\right)R_P^{-\frac{2}{k}} e_P^T e_P \\ &= 4\lambda_2\left(D_P^2\right)R_P^{-\frac{2}{k}} V_{eP}\end{aligned} \quad (40)$$

Therefore,

$$\begin{aligned}\dot{V}_2 &\leq -\frac{1}{2}\left(4\lambda_1\left(D_\omega^2 + C_\omega^2\right)V_{e\omega}\right)^{\frac{k}{2}} - \frac{1}{2}\left(4\lambda_2\left(D_P^2\right)V_{eP}\right)^{\frac{k}{2}} \\ &= -2^{k-1}R_\omega^{-1}\left(\lambda_1\left(D_\omega^2 + C_\omega^2\right)\right)^{\frac{k}{2}}\left(V_{e\omega}\right)^{\frac{k}{2}} - 2^{k-1}R_P^{-1}(\lambda_2(D_P^2)^{\frac{k}{2}}\left(V_{eP}\right)^{\frac{k}{2}}\end{aligned} \quad (41)$$

Regarding to Eq. (20), the limited time stability of the frequency and active power control can be obtained by setting $T = \max\{T_\omega, T_P\}$

$$\begin{aligned}T_\omega &= \frac{R_\omega V_{e\omega}(e_\omega(0))^{1-\frac{k}{2}}}{2^{k-1}\left(\lambda_1\left(D_\omega^2 + C_\omega^2\right)\right)^{\frac{k}{2}}\left(1-\frac{k}{2}\right)} \\ &= \frac{2^{2-k}R_\omega V_{e\omega}(e_\omega(0))^{1-\frac{k}{2}}}{(2-k)\left(\lambda_1\left(D_\omega^2 + C_\omega^2\right)\right)^{\frac{k}{2}}} \\ T_P &= \frac{2^{2-k}R_P V_{eP}(e_P(0))^{1-\frac{k}{2}}}{(2-k)\left(\lambda_2 D_P^2\right)^{\frac{k}{2}}}\end{aligned} \quad (42)$$

The block diagram of the first level of distributed control is shown in Fig. 2.

III. OPTIMAL SECONDARY CONTROL

This layer is designed to improve the transient state caused by perturbations. The system diagram shown in Fig. 3 is used to obtain the dynamic equations of the system.

According to Fig. 3,

$$\begin{aligned}v_{t,abc} &= L_t\frac{di_{t,abc}}{dt} + R_{t*}i_{t,abc} + V_{abc} \\ i_{t,abc} &= C\frac{dv_{abc}}{dt} + i_{L,abc} + \frac{v_{abc}}{R} \\ v_{abc} &= L\frac{di_{L,abc}}{dt} + R_{l*}i_{L,abc}\end{aligned} \quad (43)$$

where v_t and v_{abc} are the terminal voltages as shown in Fig. 3. By converting (43) to the static form of $\alpha\beta$, the following is obtained:

$$\begin{aligned}\frac{di_{t,\alpha\beta}}{dt} &= -\frac{R_t}{L_t}i_{t,\alpha\beta} - -\frac{v_{\alpha\beta}}{L_t} + \frac{v_{t,\alpha\beta}}{L_t} \\ \frac{dv_{\alpha\beta}}{dt} &= \frac{1}{C}i_{t,\alpha\beta} - \frac{1}{RC}v_{\alpha\beta} - \frac{i_{L,\alpha\beta}}{C} \\ \frac{di_{L,\alpha\beta}}{dt} &= \frac{v_{\alpha\beta}}{L} - \frac{R_l}{L}i_{L,\alpha\beta}\end{aligned} \quad (44)$$

By transferring (44) to the synchronous reference frame, the following is obtained:

$$\frac{di_{t,dq}}{dt} + j\omega i_{t,dq} = -\frac{R_t}{L_t}i_{t,dq} - \frac{v_{dq}}{L_t} + \frac{v_{t,dq}}{L_t}$$

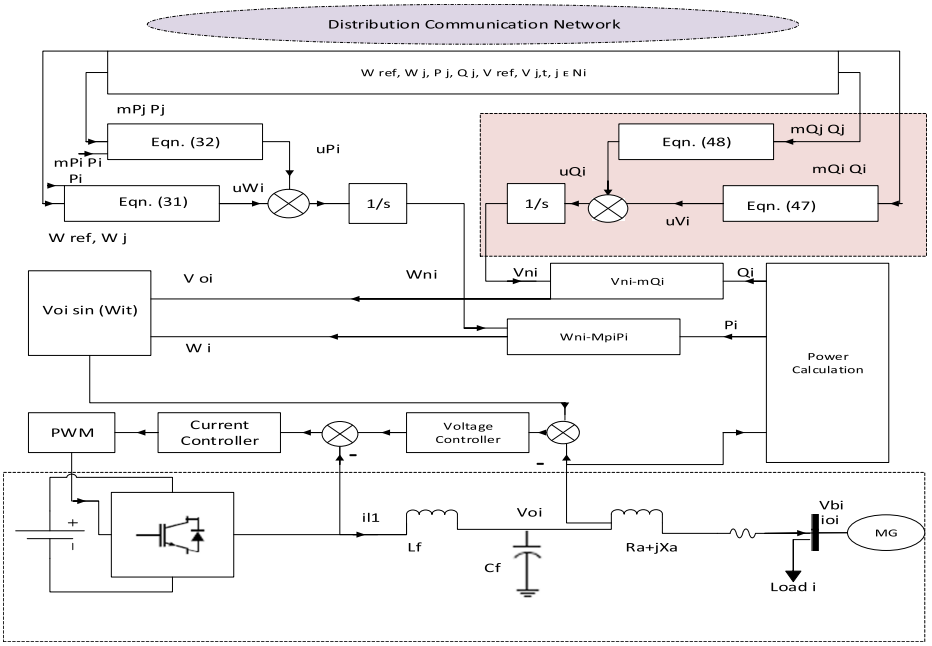

FIGURE 2. Block diagram of the first level of distributed control.

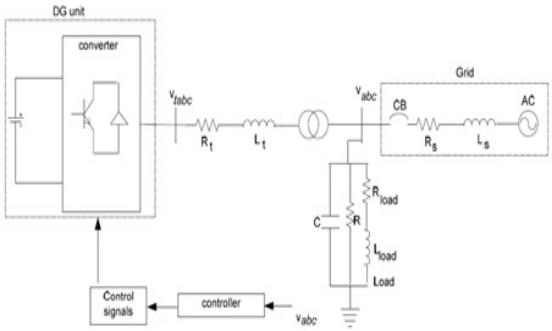

FIGURE 3. Schematic of the system used to obtain the dynamic equations for designing the PI controller.

$$\begin{aligned}\frac{dv_{dq}}{dt}+j\omega v_{dq}&=\frac{1}{C}i_{t,dq}-\frac{1}{RC}v_{dq}-\frac{i_{L,dq}}{C}\\ \frac{di_{L,dq}}{dt}+j\omega i_{L,dq}&=\frac{v_{dq}}{L}-\frac{R_l}{L}i_{L,dq}\end{aligned}\tag{45}$$

The load phase angle can be considered in such a way that v_q is equal to zero. Here dv_{dq}/dt is equal to zero, and v_d is equal to the magnitude of the load voltage. Therefore, relations (46) are as follows:

$$\begin{aligned}\frac{di_{td}}{dt}&=\omega i_{tq}-\frac{R_t}{L_t}i_{td}-\frac{v_d}{L_t}+\frac{v_{td}}{L_t}\\ \frac{dv_d}{dt}&=\frac{1}{C}i_{td}-\frac{1}{RC}v_d-\frac{i_{Ld}}{C}\\ \frac{di_{Ld}}{dt}&=\omega i_{Lq}+\frac{v_q}{L}-\frac{R_l}{L}i_{Ld}\\ \frac{di_{td}}{dt}&=-\omega i_{td}-\frac{R_t}{L_t}i_{tq}+\frac{v_{tq}}{L_t}\\ \frac{di_{tq}}{dt}&=-\omega i_{Ld}-\frac{R_l}{L}i_{Lq}\\ \omega C v_d&=i_{tq}-i_{Lq}\end{aligned}\tag{46}$$

The system state equations that can be written in matrix form are:

$$\dot{x}(t)=\mathrm{A}x(t)+\mathrm{B}u(t)y(t)=\mathrm{C}x(t)u(t)=\mathrm{D}v_t\tag{47}$$

where

$$A=\begin{bmatrix}-\frac{R_t}{L_t} & \omega_0 & 0 & -\frac{1}{L_t}\\ \omega_0 & -\frac{R_t}{L} & -2\omega_0 & \frac{R_l C\omega_0}{L_t}-\frac{\omega_0}{R}\\ 0 & \omega_0 & -\frac{R_l}{L} & \frac{1}{L}-\omega_0^2 C\\ \frac{1}{L} & 0 & -\frac{1}{C} & -\frac{1}{RC}\end{bmatrix}\tag{48}$$

$$\begin{aligned}B^T&=\begin{bmatrix}\frac{1}{L_t} & 0 & 0 & 0\end{bmatrix}\\ C&=\begin{bmatrix}0 & 0 & 0 & 1\end{bmatrix}\\ x^T&=\begin{bmatrix}i_{td} & i_{tq} & i_{Lq} & v_d\end{bmatrix}\end{aligned}\tag{49}$$

To obtain the objective function, the characteristics of the step response are considered, *i.e.*, the settling time and the maximum overshoot and undershoot according to the transfer function. Furthermore, considering the poles of the system, a stability margin criterion for the system is considered, and balances between these three values are found. Therefore, the objective function is defined as follows:

$$Z=(W_1*MP)+(W_2*Ts)+(W_3*SI)\tag{50}$$

where MP is the maximum value of the overshoot and undershoot, and Ts is the settling time. Also, the sum of weighting coefficients is determined according to the importance of each of the above, which is equal to 1. In this study, the level of importance is considered equal. SI is also an indicator of

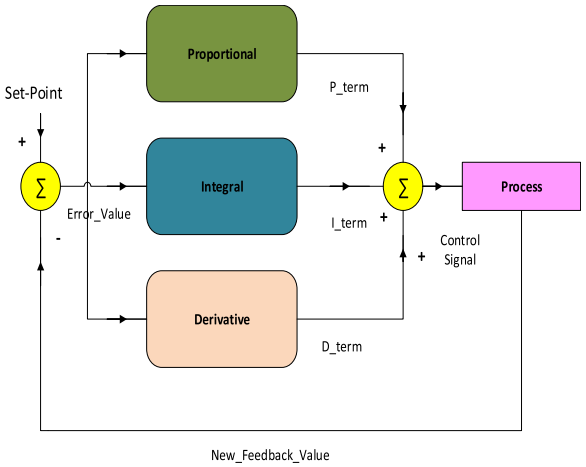

FIGURE 4. Schematic of the PID controller.

stability. The PID controller used for the secondary control is optimized by means of algorithms [24]. The schematic of this controller shown in Fig. 4.

Considering the transfer function as:

$$G(s) = \frac{B(s)}{A(s)} \tag{51}$$

and ideal PID controller (as shown in fig. 4):

$$C(s) = kp + \frac{k_I}{s} + k_D s = \frac{k_p s + k_I + k_D s^2}{s} \tag{52}$$

The substitution $s = j\omega$ and subsequent decomposition of the numerator and denominator into their even and odd parts lead to:

$$G(jw) = \frac{B_E\left(-\omega^2\right) + j\omega B_o(-\omega^2)}{A_E\left(-\omega^2\right) + j\omega A_o(-\omega^2)} \tag{53}$$

Then, the expression of closed-loop characteristic polynomial and equaling the real and imaginary parts to zero result in the relations for proportional and integral gains:

$$k_P(\omega, k_D) = \frac{P_5(\omega) P_4(\omega) - P_6(\omega) P_2(\omega)}{P_1(\omega) P_4(\omega) - P_2(\omega) P_3(\omega)} \tag{54}$$

$$k_I(\omega, k_D) = \frac{P_6(\omega) P_1(\omega) - P_5(\omega) P_3(\omega)}{P_1(\omega) P_4(\omega) - P_2(\omega) P_3(\omega)} \tag{55}$$

where

$$P_1(\omega) = -\omega^2 B_o\left(-\omega^2\right) \tag{56}$$

$$P_2(\omega) = B_E\left(-\omega^2\right) \tag{57}$$

$$P_3(\omega) = \omega B_E\left(-\omega^2\right) \tag{58}$$

$$P_4(\omega) = \omega B_o\left(-\omega^2\right) \tag{59}$$

$$P_5(\omega) = \omega^2 A_o\left(-\omega^2\right) + \omega^2 B_E\left(-\omega^2\right) k_D \tag{60}$$

$$P_6(\omega) = \omega^2 A_E\left(-\omega^2\right) + \omega^3 B_o\left(-\omega^2\right) k_D \tag{61}$$

Simultaneous solution of equations (54) and (55) leads to the stability boundary locus. So, it can be seen that the PID coefficients are effective on the stability limits.

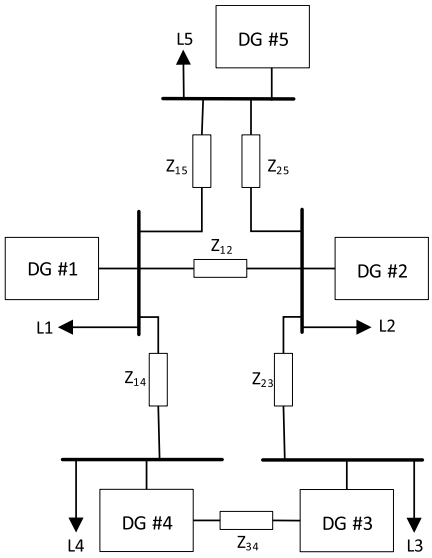

FIGURE 5. Schematic of the system under study.

To provide stability conditions, one method is to use the Hermite-Biehler theory. Equation (51) can be written as follows:

$$G(s) = \frac{k}{s(\tau s + 1)} e^{-\theta s} \tag{62}$$

where k, τ and θ are assumed to be positive. Assuming C(s) as the controller and G(s) as the plant under study, the characteristic equation of the closed loop system is [25]:

$$\delta(s) = s^2(\tau s + 1) + \left(kk_i + kk_p s + kk_d s^2\right) e^{-\theta s} \tag{63}$$

By converting (63) into quasi-polynomial:

$$f(s) = \delta(s) e^{-\theta s} = kk_i + kk_p s + kk_d s^2 + s^2(\tau s + 1) e^{\theta s} \tag{64}$$

According to (64) the stability of the system is equivalent to the condition that all the zeros of $f(s)$ are in open left-half plane.

By substituting $s = j\omega$ into (64) and taking $z = \theta\omega$, the equation in proposed system is difficult to be solved analytically. Diagramming methods and simulations are usually used for investigation. In this paper, increasing the stability range as one of the parts of the objective function has been measured by the algorithm and by valuing the coefficients of the PID controller.

On the other hand, the root locus can be used to evaluate the stability of the system, and the critical damping ratio, which is determined according to this root distribution, is an evaluation of the system robustness against disturbance, such as the load variation. The stability and robustness of microgrid will be impacted or even destructed by the coefficients of PID controller. As the stability margin increases more and more, the probability of the system working robustly increases. This is one of the goals specified in the cost function (51) function. Considered scenarios are also severe load changes and

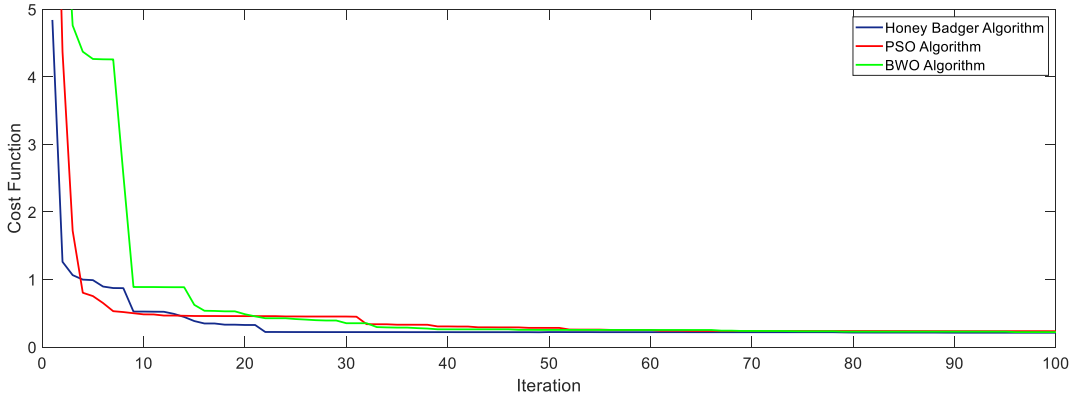

FIGURE 6. Convergence diagram for the optimization methods.

TABLE 1. System parameters.

	DG #1 and #2	3.0kW+1.5 kvar	DG #3, #4 and #5	2.0kW+1.0 kvar
DGs	m_P	$5*10^{-5}$	m_P	$6.5*10^{-5}$
	m_Q	$6*10^{-4}$	m_Q	$8*10^{-4}$
	Z_c	0.04+j0.25 Ω	Z_c	0.03+j0.15 Ω
	L_f	1.5 mH	L_f	1.5 mH
	C_f	47 µF	C_f	47 µF
Lines	Z_{14}& Z_{25}	0.05+j0.15 Ω	Z_{15}& Z_{15}	0.04+j0.1 Ω
	Z_{34}	0.08+j0.2 Ω	Z_{34}	0.1+j0.25 Ω
Loads	L_1	1.5 kW+1.5 kvar	L_3 & L_4	2.0 kW+0.5 kvar
	L_2	2.5kW+0.8 kvar	L_5	1.0 kW+1.2 kvar

TABLE 2. System load and fault scenarios.

Num	Scenario	Second
1	Starting up	0
2	50% increase in active power and 10% in reactive power demands	0.5
3	65% increase in active power and 15% in reactive power demands	1
4	40% increase in active power and 10% in reactive power demands	1.5
5	3 phase short circuit error	2

TABLE 3. Adjustment coefficients of algorithms and results.

PSO	BWO	Honey Badger
Number of iterations = 100	**Number of iterations = 100**	Number of iterations = 100
Swarm size = 15	Population size = 15	Population size = 15
Search velocity factor = 12%	Procreating rate = 0.6	A honey badger's ability to get food = 6
Velocity damping factor = 0.8	Cannibalism rate = 0.41	
Local fitness significance factor = 1.5	Mutation rate = 0.3	
Global fitness significance factor = 1.5		
	Results	
PSO Algorithm	**BWO Algorithm**	**Honey Badger Algorithm**
Proportional parameter = 55	Proportional parameter = 52.1	Proportional parameter = 67.8
Integral parameter = 2.2	Integral parameter = 2.1	Integral parameter = 2.5
Derivative parameter = 0.2	Derivative parameter = 0.2	Derivative parameter = 0.6

3-phase short circuit error to measure the robust performance of the system.

IV. CASE STUDY AND SIMULATION RESULTS

In this section, the performance of the proposed method is examined via HBA [26] and BWO [27] and PSO. The optimization completion condition for all algorithms was 100 iterations. However, after about 60 iterations, there was no significant change in the value of the cost function. The number of initial responses was also considered the same for the algorithms. The performances were also performed in large numbers and the best ones were considered as the answer. Simulations were run in MATLAB. A 50 Hz network was considered, and the nominal output voltage of the loads is 380 volts.

The schematic of the system is shown in Fig. 5 and the system parameters in Table 1. The scenarios applied to the system are described in Table 2. Attempts were made to include severe scenarios in the system's evaluation. Table 3 shows the adjustment coefficients of the algorithms used in this paper, namely PSO, BWO and honey badger, as well as the results obtained for the second-layer controller. Convergence diagrams are shown in Fig. 6.

Fig. 6 shows that the honey badger algorithm could achieve optimal results with less iterations and performed better. The time it took for the program to obtain the answer was approximately the same due to the similarities in the initial population and the lack of complex calculations in both algorithms. However, the convergence speed of the honey badger algorithm was higher than that of the PSO and BWO

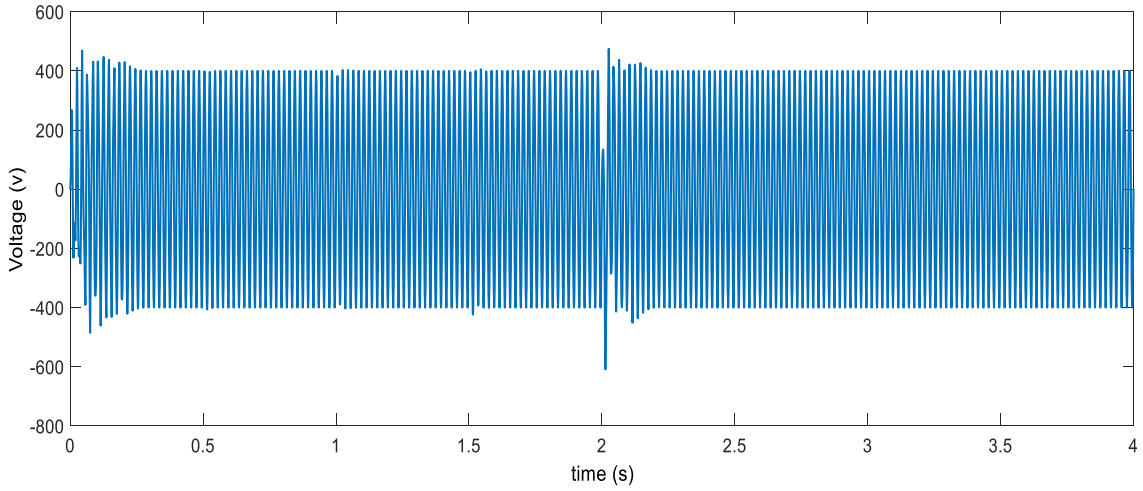

FIGURE 7. Sinusoidal voltage waveform of the loop optimized via the honey badger algorithm.

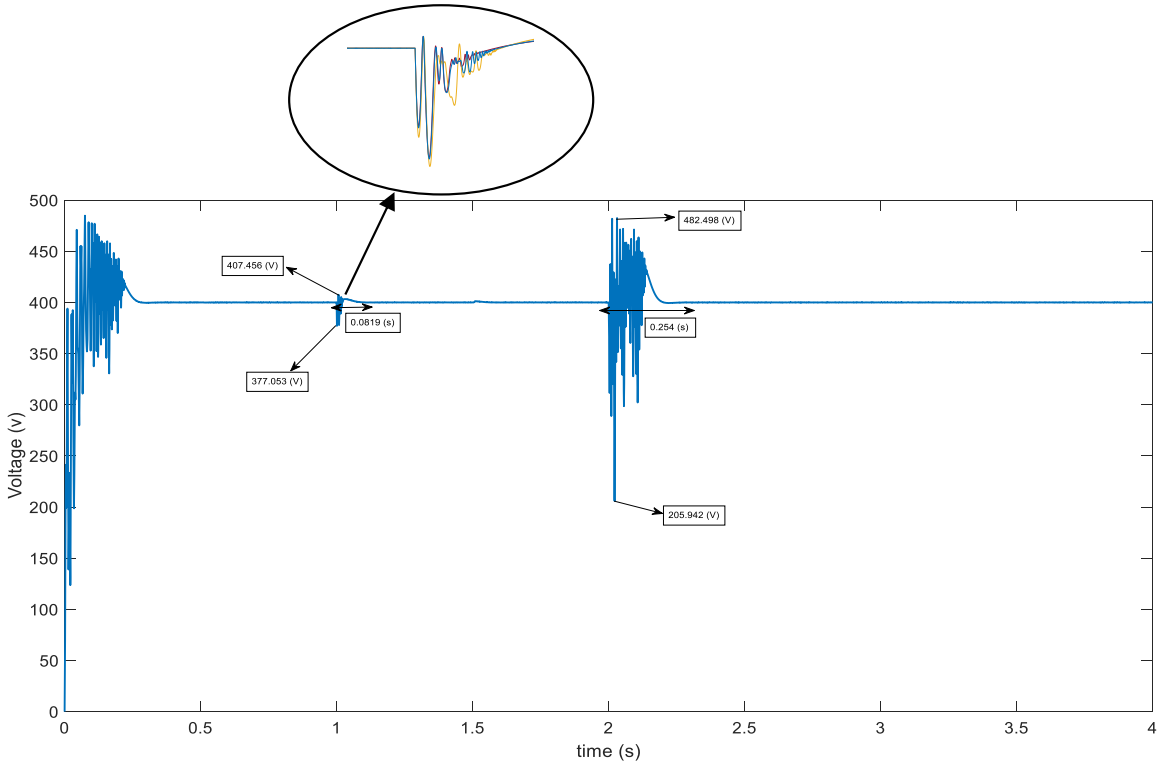

FIGURE 8. RMS voltage of the loop optimized via the honey badger algorithm.

algorithms, and a lower cost was achieved, which shows this algorithm's better solution accuracy. Moreover, in the absence of an optimal loop, the system operated with severe overshoots and undershoots, as well as with high settling times. This is evidence of poor system performance and low power quality under these conditions. This also reflects the proper functioning of the secondary control. According to Figs. 7 to 18, the following results can be inferred. With the honey badger algorithm, the least number of fluctuations was observed, and the settling time was short. With the PSO algorithm, the number of fluctuations increased dramatically. Therefore, the effect of proper optimization and application methods on minimizing the objective function is evident. These fluctuations were seen in both voltage and frequency outputs. The results for bus 1 are shown, but the results are almost the same in all buses. Figs,16 to 18 show the results for the same system without using the second control loop. In this case, the results drop sharply. Of course, the first control

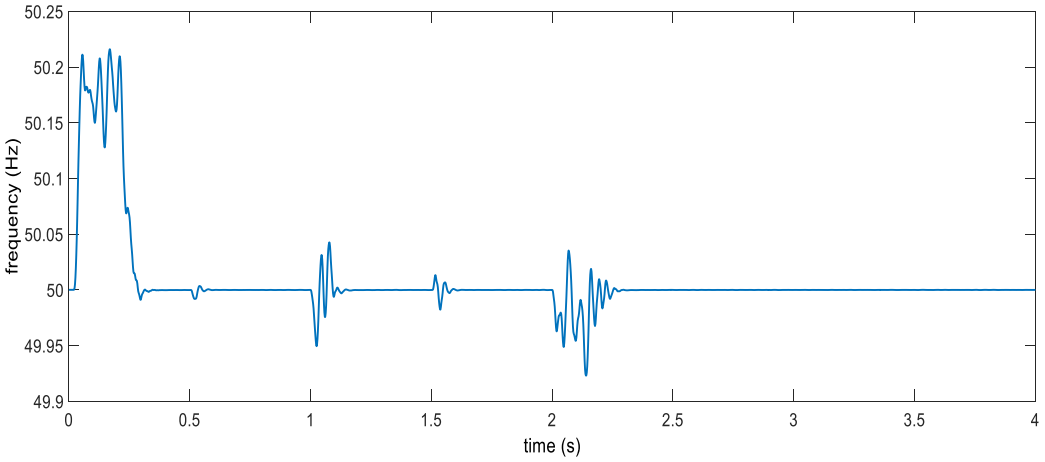

FIGURE 9. Frequency of the loop optimized via the honey badger algorithm.

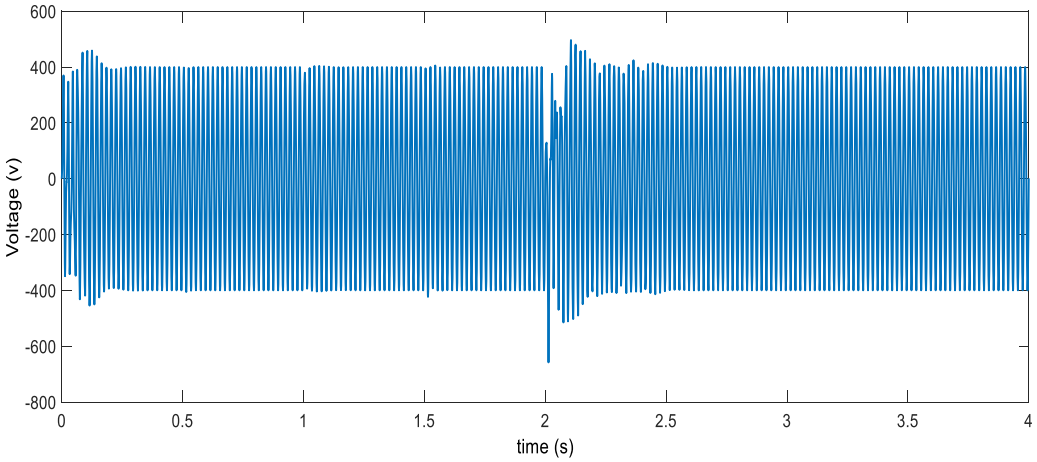

FIGURE 10. Sinusoidal voltage waveform of the loop optimized via the PSO algorithm.

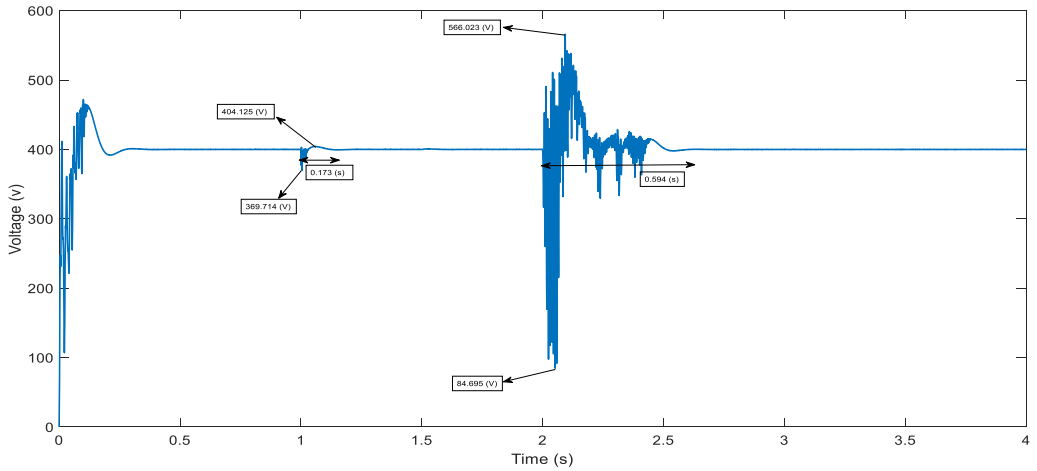

FIGURE 11. RMS voltage of the loop optimized via the PSO algorithm.

loop eventually returns the nominal values, but this is done with very low power quality. Therefore, improper adjustment of the second control level leads to poor and unacceptable results, and the appropriate power quality is not achieved.

Table 4 shows the numerical results. In using the BWO algorithm, slightly better results have been obtained than PSO. The reason for the closeness of the results of these two algorithms can be that the search method in the BWO

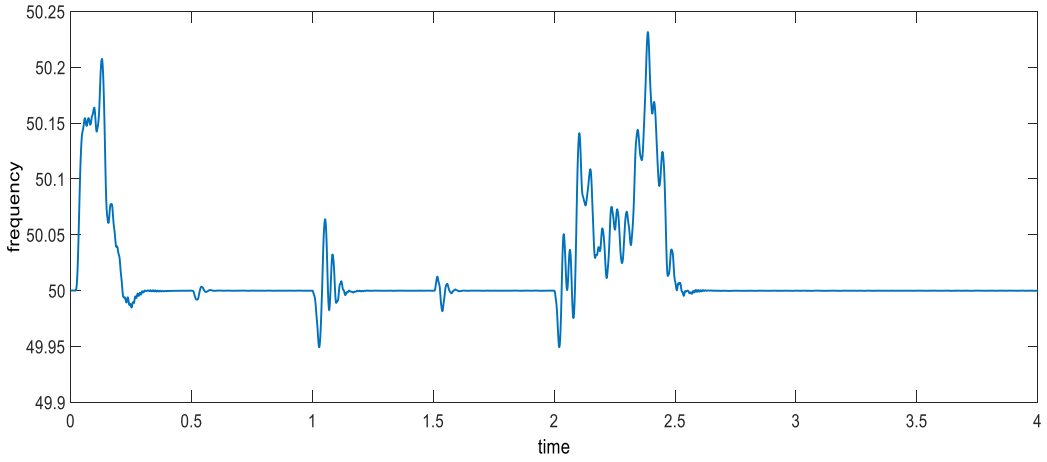

FIGURE 12. Frequency of the loop optimized via the PSO algorithm.

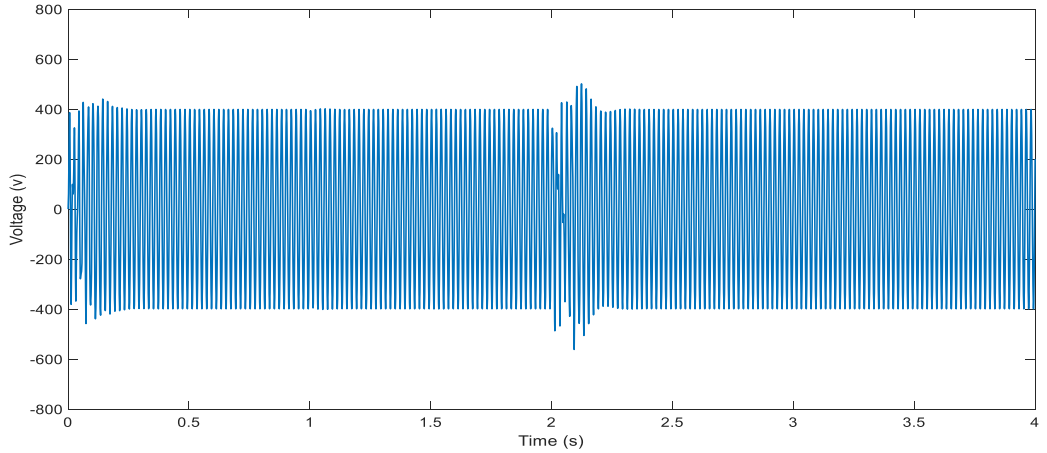

FIGURE 13. Sinusoidal voltage waveform of the loop optimized via the BWO algorithm.

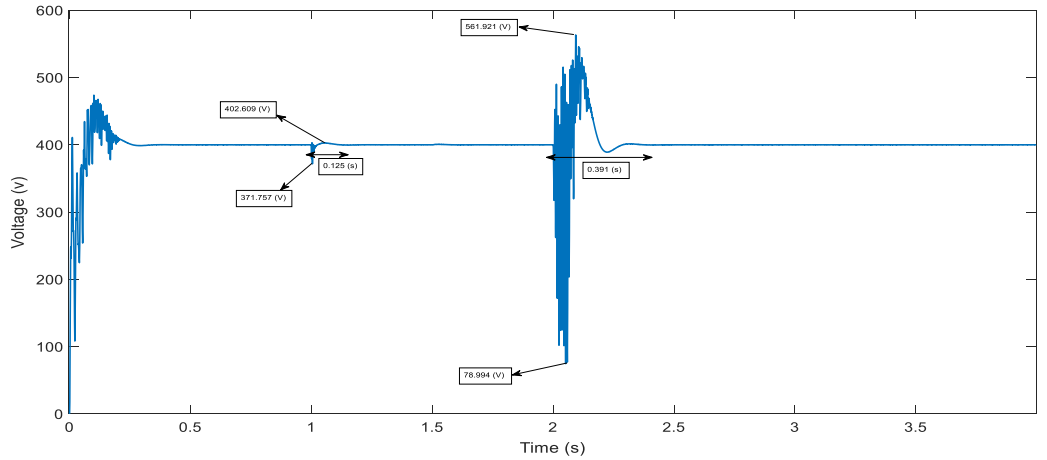

FIGURE 14. RMS voltage of the loop optimized via the BWO algorithm.

algorithm is almost similar to the Population-based algorithms. In using the HBA algorithm, the best results have been obtained (Total result in Table 4). In this method, the average maximum overshoots is 5.3%, the average minimum undershoots is 7.4%, and the average sitting time (average of all scenarios) is 0. 1686 has been obtained.

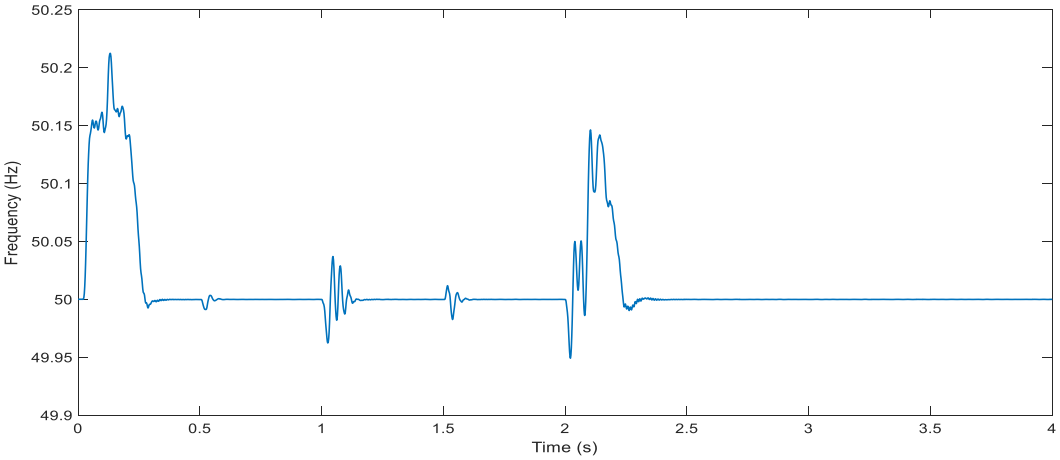

FIGURE 15. Frequency of the loop optimized via the BWO algorithm.

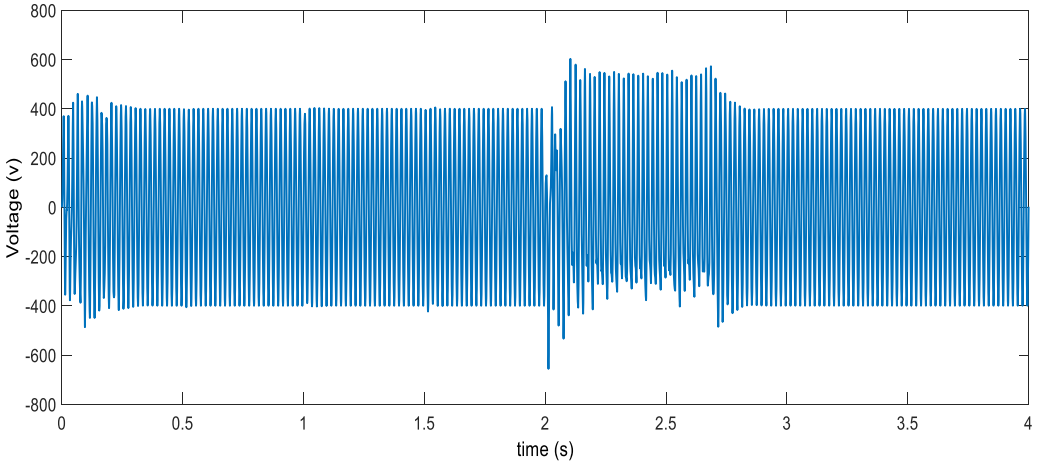

FIGURE 16. Sinusoidal voltage waveform in the absence of secondary control.

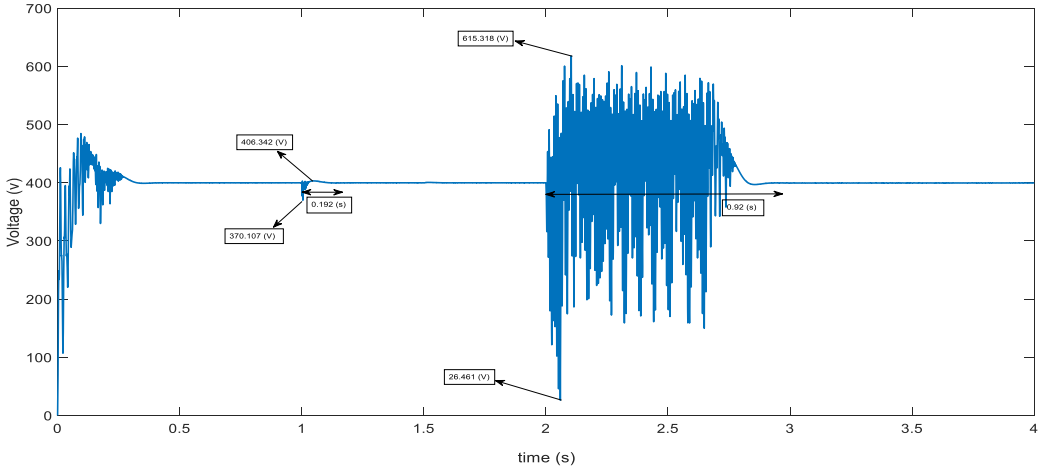

FIGURE 17. RMS voltage in the absence of secondary control.

Finally, the HBA algorithm obtained the best results. BWO and PSO algorithms had almost similar results, which reminds us that similar algorithms placed in the same category will get similar and close results. Finally, without the secondary control loop, the results were extremely poor. This comparison was made in the voltage results, which of course

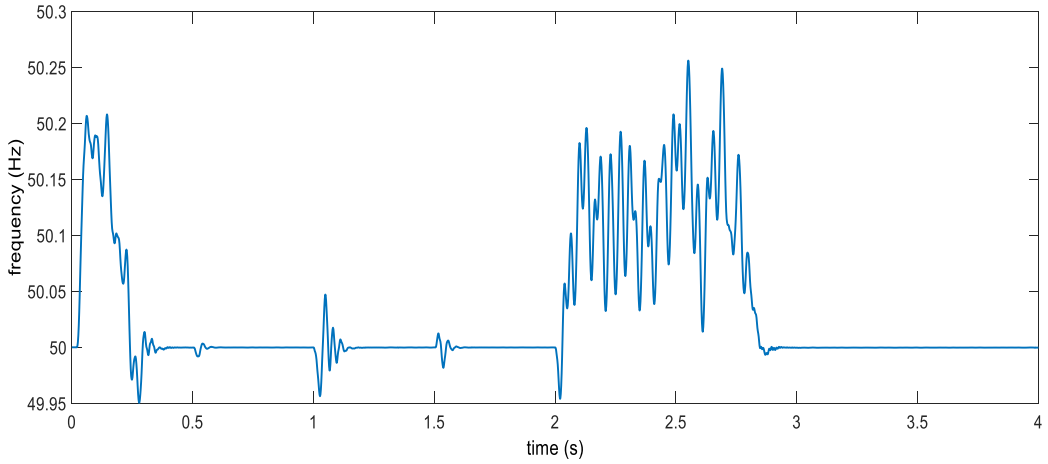

FIGURE 18. Frequency in the absence of secondary control.

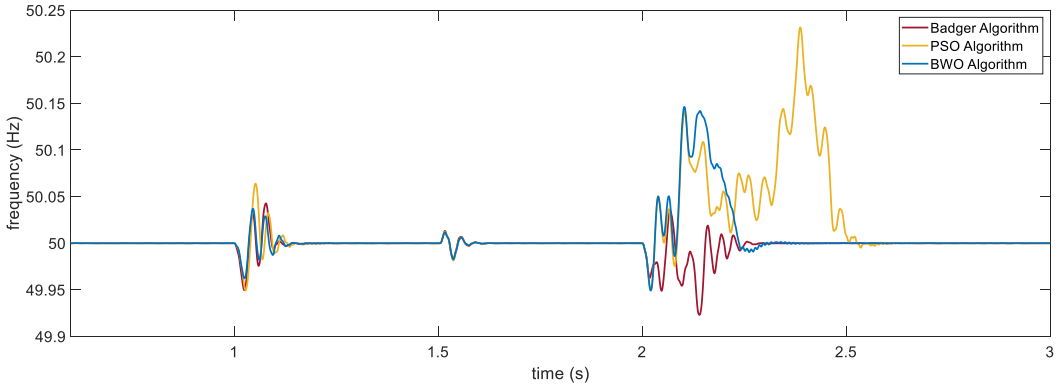

FIGURE 19. Comparison of algorithms in bus frequency output 1.

TABLE 4. Resultsof voltage for different algorithms.

Scenario number		PSO	BWO	HBA	NON
3th scenario	Max overshoot (V)	404.125	402.609	407.456	406.342
	Min undershoot (V)	369.714	371.757	377.053	370.107
	Settling time (s)	0.173	0.125	0.0819	0.192
5th scenario	Max overshoot (V)	566.023	561.921	482.498	615.318
	Min undershoot (V)	84.695	78.994	205.942	26.461
	Settling time (s)	0.594	0.391	0.254	0.92
Total result	Overshoot (%)				
	Undershoot (%)				
	Settling time (s)	0.3842	0.261	0.1686	0.561

affects the frequency and current output. Also, in examining the worst cases, it can be seen that the PSO algorithm has performed about 7% better than the BWO in obtaining the minimum undershoot in the 5th scenario. But in general and the average performance of BWO has been better.

Considering the favorable results obtained by the HBA algorithm, it may be concluded that the category of meta-heuristic algorithms with the Trajectory search method probably perform better in this category of articles.

It should be noted that the results of only one phase are shown. Since the system is balanced, the coefficients obtained for the PID controller are the same for all 3 phases. The outputs are almost constant and there is a slight difference due to the phase difference as shown in Fig. 8. Also if the coefficients of the algorithms are adjusted according to what was explained in table 3, the same results will be obtained.

V. CONCLUSION

In this paper, an integrated two-level control method was presented, whose purpose is achieving high-quality operation in microgrids. In the first level, a control based on the mathematical equations of the system and the droop controls were introduced. The second control level was entrusted to a PID controller optimized via the honey badger algorithm. The results showed that the proposed method was able to effectively control the occurrence of severe system disturbances. The power quality in the case of the honey badger algorithm was much better when compared to that of the PSO and BWO algorithms. It was also shown that not using

the second control level wields very poor and unacceptable results.

REFERENCES

[1] B. Sadeghi, N. Shafaghatian, R. Alayi, M. E. H. Assad, F. Zishan, and H. Hosseinzadeh, "Optimization of synchronized frequency and voltage control for a distributed generation system using the black widow optimization algorithm," *Clean Energy*, vol. 6, no. 1, pp. 869–882, Feb. 2022, doi: 10.1093/ce/zkab062.

[2] N. Shafaghatian, A. Kiani, N. Taheri, Z. Rahimkhani, and S. S. Masoumi, "Damping controller design based on FO-PID-EMA in VSC HVDC system to improve stability of hybrid power system," *J. Central South Univ.*, vol. 27, no. 2, pp. 403–417, Feb. 2020, doi: 10.1007/s11771-020-4305-2.

[3] M. A. Prakasa and S. Subiyanto, "Optimal cost and feasible design for grid-connected microgrid on campus area using the robust-intelligence method," *Clean Energy*, vol. 6, no. 1, pp. 823–840, Feb. 2022.

[4] M. U. Mutarraf, Y. Terriche, M. Nasir, Y. Guan, C.-L. Su, J. C. Vasquez, and J. M. Guerrero, "A communication-less multimode control approach for adaptive power sharing in ship-based seaport microgrid," *IEEE Trans. Transport. Electrific.*, vol. 7, no. 4, pp. 3070–3082, Dec. 2021, doi: 10.1109/TTE.2021.3087722.

[5] P. Vorobev, P.-H. Huang, M. A. Hosani, J. L. Kirtley, and K. Turitsyn, "Plug- and-play compliant control for inverter-based microgrids," in *Proc. IEEE Power Energy Soc. Gen. Meeting (PESGM)*, Jan. 2020, p. 1, doi: 10.1109/PESGM41954.2020.9281957.

[6] D. Zhang and E. Ambikairajah, "De-coupled PQ control for operation of islanded microgrid," in *Proc. Australas. Universities Power Eng. Conf. (AUPEC)*, Sep. 2015, pp. 1–6, doi: 10.1109/AUPEC.2015.7324820.

[7] F. Chishti, S. Murshid, and B. Singh, "Robust normalized mixed-norm adaptive control scheme for PQ improvement at PCC of a remotely located Wind–Solar PV-BES microgrid," *IEEE Trans. Ind. Informat.*, vol. 16, no. 3, pp. 1708–1721, Mar. 2020, doi: 10.1109/TII.2019.2923641.

[8] T. Caldognetto and P. Tenti, "Microgrids operation based on master–slave cooperative control," *IEEE J. Emerg. Sel. Topics Power Electron.*, vol. 2, no. 4, pp. 1081–1088, Dec. 2014, doi: 10.1109/JESTPE.2014.2345052.

[9] S. Sivaranjani, E. Agarwal, V. Gupta, P. Antsaklis, and L. Xie, "Distributed mixed voltage angle and frequency droop control of microgrid interconnections with loss of distribution-PMU measurements," *IEEE Open Access J. Power Energy*, vol. 8, pp. 45–56, 2021, doi: 10.1109/OAJPE.2020.3047639.

[10] A.-C. Braitor, G. C. Konstantopoulos, and V. Kadirkamanathan, "Current-limiting droop control design and stability analysis for paralleled boost converters in DC microgrids," *IEEE Trans. Control Syst. Technol.*, vol. 29, no. 1, pp. 385–394, Jan. 2021, doi: 10.1109/TCST.2019.2951092.

[11] B. Liu, T. Wu, Z. Liu, and J. Liu, "A small-AC-signal injection-based decentralized secondary frequency control for droop-controlled islanded microgrids," *IEEE Trans. Power Electron.*, vol. 35, no. 11, pp. 11634–11651, Nov. 2020, doi: 10.1109/TPEL.2020.2983878.

[12] Y. Ling, Y. Li, Z. Yang, and J. Xiang, "A dispatchable droop control method for distributed generators in islanded AC microgrids," *IEEE Trans. Ind. Electron.*, vol. 68, no. 9, pp. 8356–8366, Sep. 2021, doi: 10.1109/TIE.2020.3013547.

[13] D. Choi, J.-W. Park, and S. H. Lee, "Virtual multi-slack droop control of stand-alone microgrid with high renewable penetration based on power sensitivity analysis," *IEEE Trans. Power Syst.*, vol. 33, no. 3, pp. 3408–3417, May 2018, doi: 10.1109/TPWRS.2018.2810443.

[14] Z. Wang, S. Qiu, R. Song, X. Wang, B. Zhu, and B. Li, "Research on PID parameter tuning of coordinated control for ultra-supercritical units based on ziegler nichols method," in *Proc. IEEE 3rd Adv. Inf. Manage., Communicates, Electron. Autom. Control Conf. (IMCEC)*, Oct. 2019, pp. 1155–1158, doi: 10.1109/IMCEC46724.2019.8984069.

[15] M. M. Sayed, M. S. Saad, H. M. Emara, and E. E. Abou El-Zahab, "A novel method for tuning the PID parameters based on the modified biogeography-based optimization for hydraulic servo control system," in *Proc. 6th IET Int. Conf. Power Electron., Mach. Drives (PEMD)*, 2012, pp. 1–5, doi: 10.1049/cp.2012.0171.

[16] B. Alghamdi and C. A. Canizares, "Frequency regulation in isolated microgrids through optimal droop gain and voltage control," *IEEE Trans. Smart Grid*, vol. 12, no. 2, pp. 988–998, Mar. 2021, doi: 10.1109/TSG.2020.3028472.

[17] R. Mahmud, M. A. Hossain, and H. Pota, "Nonlinear output feedback droop control for parallel inverters in standalone microgrids," in *Proc. 9th Int. Conf. Power Energy Syst. (ICPES)*, Dec. 2019, pp. 1–6, doi: 10.1109/ICPES47639.2019.9105385.

[18] J. F. Patarroyo-Montenegro, F. Andrade, J. M. Guerrero, and J. C. Vasquez, "A linear quadratic regulator with optimal reference tracking for three-phase inverter-based islanded microgrids," *IEEE Trans. Power Electron.*, vol. 36, no. 6, pp. 7112–7122, Jun. 2021, doi: 10.1109/TPEL.2020.3036594.

[19] R. Alayi, F. Zishan, M. Mohkam, S. Hoseinzadeh, S. Memon, and D. A. Garcia, "A sustainable energy distribution configuration for microgrids integrated to the national grid using back-to-back converters in a renewable power system," *Electronics*, vol. 10, no. 15, p. 1826, Jul. 2021.

[20] X. Dong, X. Li, and S. Cheng, "Energy management optimization of microgrid cluster based on multi-agent-system and hierarchical Stackelberg game theory," *IEEE Access*, vol. 8, pp. 206183–206197, 2020, doi: 10.1109/ACCESS.2020.3037676.

[21] Y. Xu, H. Sun, W. Gu, Y. Xu, and Z. Li, "Optimal distributed control for secondary frequency and voltage regulation in an islanded microgrid," *IEEE Trans. Ind. Informat.*, vol. 15, no. 1, pp. 225–235, Jan. 2019, doi: 10.1109/TII.2018.2795584.

[22] M. Ross, C. Abbey, F. Bouffard, and G. Joos, "Multiobjective optimization dispatch for microgrids with a high penetration of renewable generation," *IEEE Trans. Sustain. Energy*, vol. 6, no. 4, pp. 1306–1314, Oct. 2015, doi: 10.1109/TSTE.2015.2428676.

[23] W. Yuan, Y. Wang, and Z. Chen, "New perspectives on power control of AC microgrid considering operation cost and efficiency," *IEEE Trans. Power Syst.*, vol. 36, no. 5, pp. 4844–4847, Sep. 2021, doi: 10.1109/TPWRS.2021.3080141.

[24] R. Alayi, F. Zishan, S. R. Seyednouri, R. Kumar, M. H. Ahmadi, and M. Sharifpur, "Optimal load frequency control of island microgrids via a PID controller in the presence of wind turbine and PV," *Sustainability*, vol. 13, no. 19, p. 10728, Sep. 2021, doi: 10.3390/su131910728.

[25] L. Ou, Y. Tang, D. Gu, and W. Zhang, "Stability analysis of PID controllers for integral processes with time delay," in *Proc. Amer. Control Conf.*, Jun. 2005, pp. 4247–4252, doi: 10.1109/ACC.2005.1470646.

[26] F. A. Hashim, E. H. Houssein, K. Hussain, M. S. Mabrouk, and W. Al-Atabany, "Honey badger algorithm: New Metaheuristic algorithm for solving optimization problems," *Math. Comput. Simul.*, vol. 192, pp. 84–110, Feb. 2022, doi: 10.1016/j.matcom.2021.08.013.

[27] V. Hayyolalam and A. A. P. Kazem, "Black widow optimization algorithm: A novel meta-heuristic approach for solving engineering optimization problems," *Eng. Appl. Artif. Intell.*, vol. 87, Jan. 2020, Art. no. 103249, doi: 10.1016/j.engappai.2019.103249.

EHSAN AKBARI was born in Borujerd, Iran, in 1987. He received the B.Sc. and M.Sc. degrees in power electrical engineering from the Mazandaran University of Science and Technology (MUST), Babol, Iran, in 2010 and 2014, respectively. His research interests include power quality and distribution flexible AC transmission systems (DFACTSs), application of power electronics in power systems, power electronics multilevel converters, Smart grids, harmonics, reactive power control using hybrid filters, and renewable energy systems. He has published more than 125 papers in reputed journals and conferences. He is a Contributing Reviewer of *AJEEE Journal*.

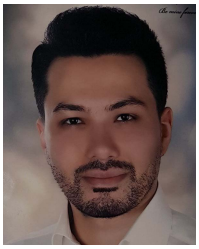

NIMA SHAFAGHATIAN received the M.S. degree from Zanjan University, where he is currently pursuing the Ph.D. degree. He has authored several articles published by IET, Springer, and other well-known publishers. He has also published two books on renewable energy and the relationship between industry and academia subjects. He is a Lecturer with Al-Ghadir University, Zanjan, and offers courses in electrical installations, smart home design, and specialized language of electricity. His research interests include microgrids, distributed generation, and electricity market.

FARHAD ZISHAN was born in Ardabil, Iran, in 1985. He received the B.Sc. degree in electrical power engineering from Islamic Azad University, Ardabil, Iran, in 2014, and the M.Sc. degree in electrical power system, in 2017. He is currently pursuing the Ph.D. degree in power electricity with the Sahand University of Technology. His research interests include renewable energy, distributed generation, optimization, power systems, and electronics.

OSCAR DANILO MONTOYA was born in Obando, Valle, Colombia, in 1989. He received the B.E.E., M.Sc., and Ph.D. degrees in electrical engineering from the Universidad Tecnológica de Pereira, Colombia, in 2012, 2014, and 2019, respectively. He is currently an Assistant Professor in electrical engineering programs with Universidad Distrital Francisco José de Caldas and the Universidad Tecnológica de Bolívar, Colombia. His research interests include mathematical optimization, planning and control of power systems, renewable energies, energy storage, protective devices, passivity-based control, and dynamical analysis.

DIEGO ARMANDO GIRAL-RAMÍREZ was born in Bogotá, Colombia. He received the undergraduate and master's degrees in electrical engineering. He is currently pursuing the doctoral degree in engineering with the Universidad Distrital Francisco José de Caldas, Colombia. He is an Assistant Professor of electrical engineering programs with Universidad Distrital Francisco José de Caldas. His research interests include mathematical optimization, automation, and intelligent systems.